eScience 4 (2024) 100280

Contents lists available at ScienceDirect

eScience

journal homepage: www.keaipublishing.com/en/journals/escience

Research Paper

Investigating explainable transfer learning for battery lifetime prediction under state transitions

Tianze Lin [a,b,1], Sihui Chen [a,b,c,1], Stephen J. Harris [d], Tianshou Zhao [b,c], Yang Liu [e,*], Jiayu Wan [a,b,c,f,*]

[a] Global Institute of Future Technology, Shanghai Jiao Tong University, No. 800 Dongchuan Road, Shanghai 200240, China
[b] Department of Mechanical and Energy Engineering, Southern University of Science and Technology, Shenzhen 518055, China
[c] SUSTech Energy Institute for Carbon Neutrality, Southern University of Science and Technology, Shenzhen 518055, China
[d] Energy Storage and Distributed Resources Division, Lawrence Berkeley National Lab, Berkeley, CA 94720, USA
[e] Data Science Research Center, Duke Kunshan University, No. 8 Duke Avenue, Kunshan 215316, China
[f] Center for Advanced Energy System and Reliability, Shanghai Jiao Tong University, No. 800 Dongchuan Road, Shanghai 200240, China

HIGHLIGHTS

- Transfer learning is leveraged to accommodate the state transition issue in battery lifetime prediction.
- Two novel transfer learning methods are proposed to effectively utilize data with variations in accessibility.
- Experimental results demonstrate that the proposed method outperforms baselines by up to 41%.
- The proposed methods demonstrate strong explainability to uncover the electrochemical principals behind state transition.

GRAPHICAL ABSTRACT

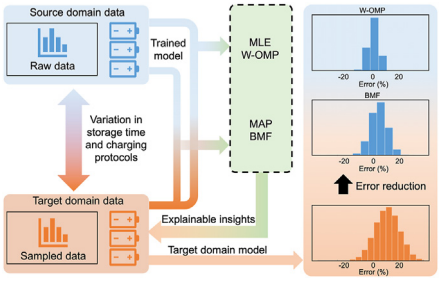

ARTICLE INFO

Keywords:
Battery life prediction
Transfer learning
State transitions
Explainability
Degradation mechanism

ABSTRACT

Battery lifetime prediction at early cycles is crucial for researchers and manufacturers to examine product quality and promote technology development. Machine learning has been widely utilized to construct data-driven solutions for high-accuracy predictions. However, the internal mechanisms of batteries are sensitive to many factors, such as charging/discharging protocols, manufacturing/storage conditions, and usage patterns. These factors will induce state transitions, thereby decreasing the prediction accuracy of data-driven approaches. Transfer learning is a promising technique that overcomes this difficulty and achieves accurate predictions by jointly utilizing information from various sources. Hence, we develop two transfer learning methods, Bayesian Model Fusion and Weighted Orthogonal Matching Pursuit, to strategically combine prior knowledge with limited information from the target dataset to achieve superior prediction performance. From our results, our transfer learning methods reduce root-mean-squared error by 41% through adapting to the target domain. Furthermore, the transfer learning strategies identify the variations of impactful features across different sets of batteries and therefore disentangle the battery degradation mechanisms and the root cause of state transitions from the perspective of data mining. These findings suggest that the transfer learning strategies proposed in our work are capable of acquiring knowledge across multiple data sources for solving specialized issues.

* Corresponding authors.
E-mail addresses: yang.liu2@dukekunshan.edu.cn (Y. Liu), wanjy@sjtu.edu.cn (J. Wan).
[1] These authors contributed equally to this work.

https://doi.org/10.1016/j.esci.2024.100280
Received 30 December 2023; Received in revised form 7 May 2024; Accepted 15 May 2024
Available online 21 May 2024

1. Introduction

Energy storage technology plays a prominent role on the world's sustainability and offers reliable energy sources to various real-world applications, such as consumer electronics [1–4], electric vehicles [5–7], and power grids [8–10]. Rechargeable batteries, especially Li-ion batteries (LIBs), are among of the most recognizable energy storage technologies, and they have already significantly impacted human lifestyle and industrial activities due to their excellent energy and power densities [11–14]. As rechargeable batteries will be increasingly critical in the foreseeable future, their quality and reliability are of vital importance to our society [15]. Furthermore, the close relevance of these parameters to battery lifetime [16–19] makes lifetime prediction at early cycles a crucial task for researchers and manufacturers to examine their product quality [20] and facilitate decision making on product maintenance and Research and Development (R&D) [21]. In recent years, machine learning (ML) techniques have gained significant popularity in the renewable energy domain [22,23]. Instead of the conventional electrochemical model-based approaches, machine learning has been employed to construct data-driven approaches for highly efficient lifetime prediction of rechargeable batteries [16,24,25]. A precursor in this line of research established an ElasticNet model trained using the data collected from the first 100 discharge cycles of 41 lithium-ion rechargeable batteries, which achieves a high prediction accuracy with 9.1% test error using discharge voltage curves from early cycles [26]. Inspired by the early success, a number of subsequent research papers have focused on investigating the latest developments in machine learning models for superior prediction accuracies [27–32].

Despite the above advances, there exist the following challenges that prevent the large-scale deployment of data-driven battery lifetime prediction techniques in practice. First, as the measurement of battery lifetime is usually associated with long feedback time and costly testing channels/sensors, the prediction models need to be trained using a limited amount of data samples in most scenarios, which can potentially induce overfitting and weaken the generalization capability of the models [33–37]. Second, the internal features of batteries are sensitive to multiple complex factors such as test temperature [14], charging/discharging protocols, manufacturing/storage conditions, and usage pattern (Fig. 1a) [38–42]. The variations of these external factors can induce transitions to the correlations between battery lifetime and the related measurements. Thus, the accuracy of a prediction model may substantially decrease when applied to a set of batteries other than the training dataset, even if they use the same type of batteries. This has been demonstrated in the previous study [26], where the model performs substantially worse on the secondary testing dataset (root mean square error (RMSE) $>$ 200) compared with the primary testing dataset (RMSE $>$ 100), as shown in Fig. 1b.

In order to tackle the aforementioned challenges, transfer learning, a specific strategy of machine learning that enables knowledge sharing between similar/related tasks, has been employed in several recent works to help adapt the originally trained models to fit new scenarios [43–47]. As the internal mechanisms of the widely used LIBs follow common electrochemical principles [48], different sets of batteries share strong similarities despite the potential state transitions. This makes transfer learning a natural option to update a base model trained using the data from the source domain to a new target domain through fine-tuning with limited data sampled from the new dataset. In return, transfer learning also improves the efficiency for training a model in the target domain through incorporating prior knowledge from the source domain [43,44]. Generally, transfer learning can be classified into three main categories, i.e., transductive transfer learning, inductive transfer learning, and unsupervised transfer learning. Transductive transfer learning targets the scenarios with identical tasks, but different data

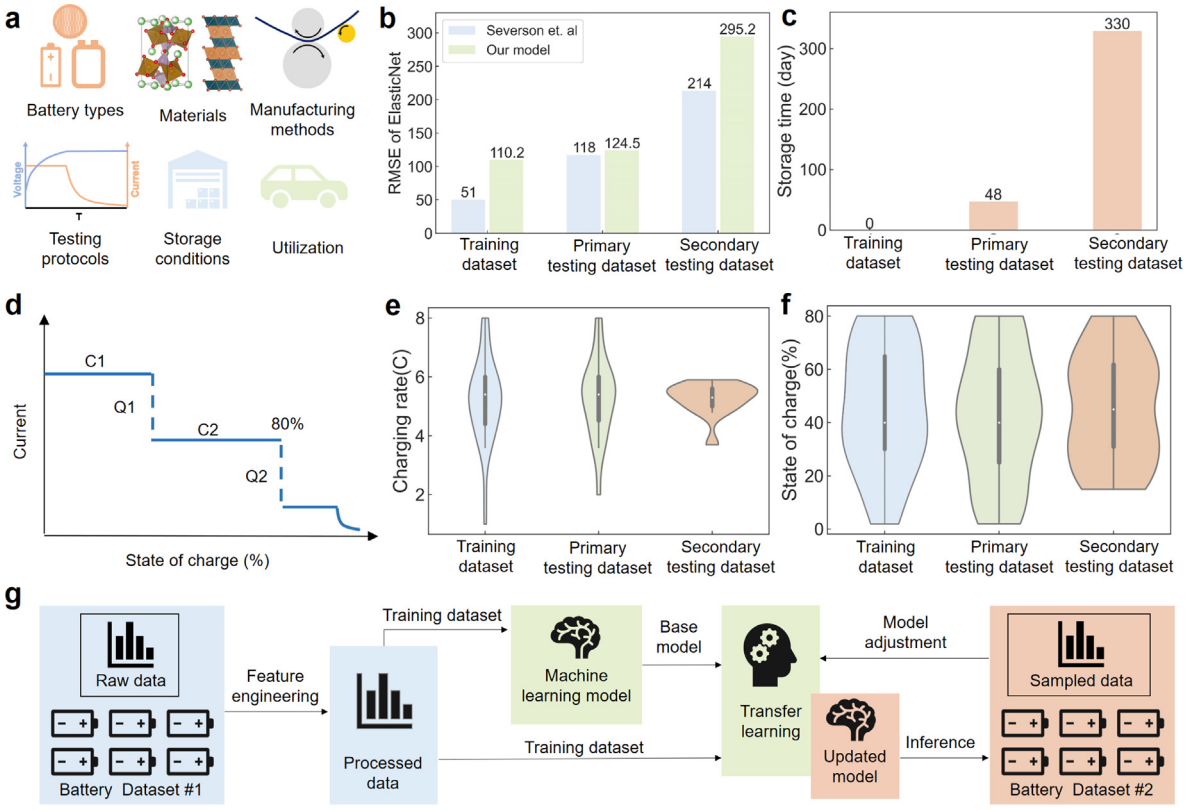

Fig. 1. Background for transfer learning in accurate battery life prediction. (a) Potential factors that would influence the cycle life of batteries. (b) The RMSE of ElasticNet from Severson *et al.* [26] and our work. (c) Storage time of each dataset. (d) Illustration of charging protocols used to obtain the datasets. C1 and C2 are the constant charging rate at the first and second step, respectively. Q1 is the State of Charge (SOC) at which the currents change, and Q2 is the SOC from current switch to 80%. (e) C1 of each dataset. (f) Q1 of each dataset. (g) Flowchart illustrating the process of the proposed transfer learning methodology.

distributions in the source and target domains. In contrast, inductive transfer learning tackles the challenges when variations exist between the tasks in source and target domains. Unsupervised transfer learning considers a similar scenario with inductive transfer learning, while the data are unlabeled in both source and target domains [49–52]. Based on these advances, impressive progress has been made in recent rechargeable battery-related research, which demonstrated that the modeling accuracy can be significantly improved through taking a peek at the target dataset via transductive transfer learning [45–47]. Apart from accuracy, explainability is another critical issue for the data-driven approaches of rechargeable battery research, since important decisions cannot be made without a solid understanding of safety and reliability. In this work, we desire to investigate the explainability of transfer learning methods. To reach this goal, transfer learning algorithms are investigated in conjunction with explainable machine learning techniques. The conclusions drawn from the aforementioned workflow are analyzed using electrochemical principles to examine the determining factors of battery lifetime during state transitions and fully discover their impact to the internal degradation mechanisms of lithium-ion batteries. This can also help us propose appropriate strategies on the design, manufacture, usage, storage, and maintenance of rechargeable batteries. However, existing research in this field primarily focuses on the enhancement of modeling accuracy provided by transfer learning, while overlooking the significance of explainability and the influence of external factors on the state transition of discharging characteristics [45–47].

In this paper, we investigate the explainability of transfer learning in addition to accuracy for battery lifetime prediction. Unlike existing research that transfers to the target task through fine-tuning the parameters of specific layers in the base model [46,47], we focus on modifying the selection and weighting of input features to efficiently evaluate the variations of impacting factors in the target domain. Furthermore, as the accessibility of prior knowledge can be different due to the real-world constraints, we consider two scenarios, where we can get access to the base model only and to the data used to train the base model, respectively. Two individual transfer learning algorithms, Bayesian Model Fusion (BMF) [53] and an innovative Weighted Orthogonal Matching Pursuit (W-OMP), are developed correspondingly for whether only the model or raw data are available in these scenarios. Compared with the base mode used in previous research [26], transfer learning models can reduce the prediction root-mean-squared error (RMSE) by up to 41% and recognize the dominant impacting factors for battery lifetime in the target domain. Additionally, leveraging data directly from the source domain for knowledge sharing is more effective than fine-tuning the base model, resulting in lower prediction errors with less data from the target domain. While most of the recent research form the prediction models based on deep learning techniques for higher prediction accuracy [46,47], our methods are established using simple linear regression-based techniques due to the following advantages: First, the proposed algorithms are efficient to implement and transparent to the researchers, such that one can seek the explainability of the prediction models and understand the impact of considered factors through directly analyzing the weights corresponding to the input features. Second, the proposed algorithms are flexible and have a strong capability for generalization. In fact, the deep learning models for battery lifetime prediction can basically be regarded as linear regression models that take the output of early layers as input features. It means that our proposed transfer learning algorithms have high potentials to be applied to deep learning models as well. Thus, the proposed models can be generalized to accommodate both handcrafted features and those extracted by deep neural networks. These advantages enable the proposed models to be more reliable for tackling the challenges in real-world scenarios.

2. Results

In order to demonstrate the capability of the developed transfer learning methods for battery lifetime prediction, we conduct our experiment using the lithium iron phosphate (LFP)/graphite open-source data from the earlier investigation [26]. For comparison, we apply the ElasticNet algorithm, which was utilized in previous work [26], as a baseline to evaluate the improvement of prediction accuracy. To ensure the efficacy of our proposed algorithms, we utilize the same features employed in the full model introduced by the precursor research [26], which utilizes nine features to predict battery cycle life. The dataset initially contains 140 batteries with 1.1 Ah nominal capacity, which are separated into three sub-datasets named training dataset, primary testing dataset, and secondary testing dataset, containing 46, 48, and 46 batteries, respectively. After removing a few irregularities for each dataset, we finally include 124 batteries, containing 41, 43, and 40 batteries for the aforementioned datasets, respectively. In the precursor research [26], although the predictive RMSE in the training and primary testing datasets are 51 and 116, respectively, it reaches 214 on the secondary testing dataset, which indicates that the effectiveness of the model can suffer from large variance across different datasets (Fig. 1b). This is validated in this paper as well through training an ElasticNet model in a similar way, where a similar pattern of predictive RMSE is achieved compared with the previous study (Fig. 1b) [26]. To understand this phenomenon, we analyzed the three datasets and found at least two inherent differences between these datasets. Firstly, the calendar aging of batteries within these datasets are different (Fig. 1c, around one-year extra storage time for secondary testing dataset), resulting in low initial capacity for the batteries of secondary testing dataset (Supplementary Fig. 1). Aging is a degradation process influenced by various factors, including battery chemistry, temperature, moisture, and time itself, regardless of whether the battery is actively cycled or stored. And it commences immediately upon battery production, and persists throughout the entire battery lifetime, encompassing storage, charging and discharging processes [54,55]. Secondly, compared with other datasets, secondary testing dataset has its unique charging protocol (Fig. 1d), reflected by a narrower distribution of initial charging rate (C1, Fig. 1e) and State of Charge (SOC) when C1 ends, which is referred to as Q1 (Fig. 1f, also see Supplementary Figs. 2 and 3). In this paper, we desire to investigate the impacts of these variations on battery lifetime prediction and explore the way to improve the modeling accuracy in these scenarios. For this purpose, we only focus on the training dataset and secondary testing dataset since the primary testing dataset has a strong similarity with the training dataset and the model trained using training dataset can achieve a sufficiently high accuracy on it.

Due to the aforementioned data variations induced by battery states transitions, a lifetime prediction model trained on a dataset can hardly achieve an equally high prediction accuracy when applied to a set of batteries with state transitions. Therefore, transfer learning is utilized to establish prediction solutions to adapt the knowledge extracted from the training dataset to fit the target testing dataset through taking a peek at it (Fig. 1g). As transfer learning is a machine learning strategy that can improve the model performance on a new task by reusing information acquired from a different but similar problem [43], it is a natural option to accommodate a potential state transitions in a wide variety of domains including battery lifetime predictions [39,56,57]. Note that the availability of information for reusing in transfer learning can be different due to practical limitations. For example, one might obtain access to the raw data used for training the base model or only to the base model itself. In this work, we investigate both situations and aim to develop distinct algorithms to explore the effective utilization of available information, as depicted in Fig. 1g. For the scenario when only a base model is accessible, we train a linear regression model with ElasticNet regularization using the training dataset [26]. Subsequently, that linear regression model is used as the base model, which is fine-tuned based on limited data samples from the secondary testing dataset using BMF [53], a specific transfer learning technique that combines the prior knowledge and late-stage observations using maximum-a-posteriori (MAP) estimation, to re-assign the weights of input features (Figs. 2a and b). In the scenario

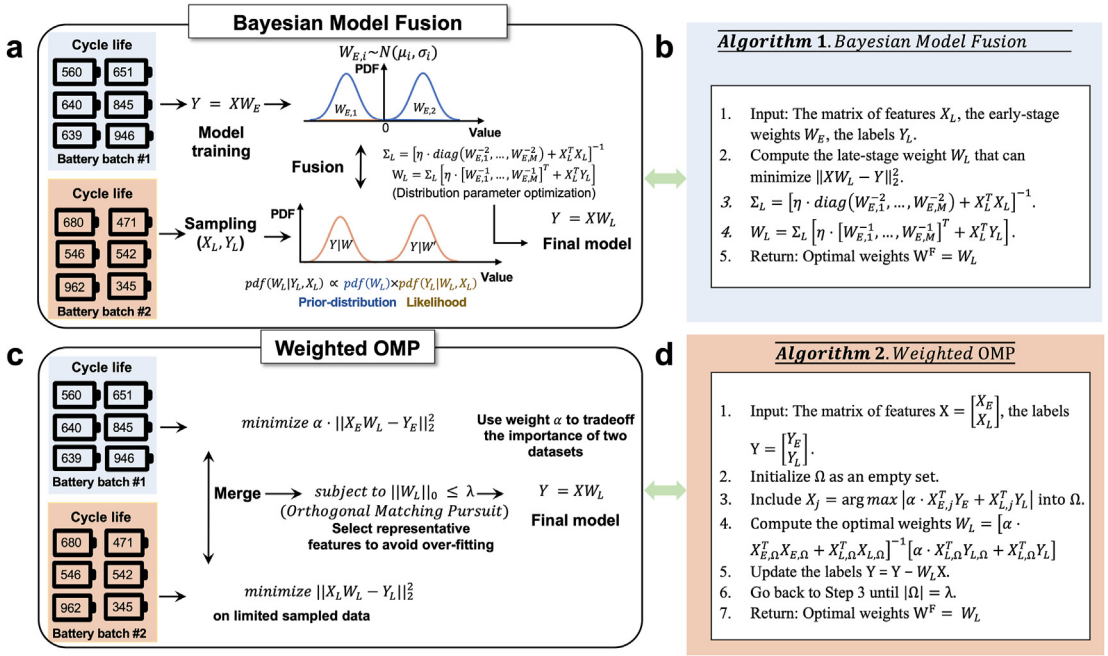

Fig. 2. Algorithm flowcharts and Pseudo codes. (a) Flowchart of the Bayesian model fusion for cycle life prediction. (b) Detailed algorithm of the Bayesian model fusion. (c) Flowchart of Weighted OMP for cycle life prediction. (d) Detailed algorithm of Weighted OMP.

where the raw dataset for training the base model is accessible, a novel W-OMP algorithm is proposed to train a linear regression model through achieving a reasonable tradeoff between training dataset and the data sampled from the testing dataset as well as selecting the impactful features (Figs. 2c and d). Since the base model is basically an encoded format of the knowledge in the training dataset, fine-tuning from the base model can potentially induce the loss of information compared to directly utilizing the training dataset, and consequently lead to inferior prediction accuracy. Hence, we expect the W-OMP method to generate more reliable prediction while BMF is more adaptable since it is not limited to the accessibility of information. The details of the transfer learning algorithms are presented in Methods section.

In order to evaluate the developed transfer learning algorithms, we randomly divide the secondary testing dataset into two parts including the developing part and testing part. The developing part consists of 10 data samples, and the testing part consists of 30 data samples where the developing part is used to draw observations from the target domain for transfer learning, and the testing part is used to evaluate the prediction accuracy. While training the transfer learning models, we increase the number of data samples drawn from developing part from 6 to 10 and compute the prediction RMSE on the testing data samples for each case. We compare with two baseline algorithm including the ElasticNet algorithm used in the previous research [26] and the Orthogonal Matching Pursuit (OMP) algorithm [58] based on the prediction RMSE on the test part of the secondary testing dataset. Both these algorithms can effectively train a linear regression model using limited number of data samples while OMP is proven to be more reliable when the problem is highly under-determined due to the strict L0-norm regularization, which poses a constraint on the number of non-zero features included in the model. The ElasticNet algorithm is purely trained using the training dataset to match the scenario in earlier investigation [26] and the OMP algorithm is trained using the data drawn from the developing part. Similar to the transfer learning algorithms, we increase the number of developing data samples for training OMP from 6 to 10 and compute the prediction RMSE for each case. Note that ElasticNet and OMP fit the prediction models based on the information individually from the training and secondary testing datasets, respectively. We would like to compare with these baselines to demonstrate the advantages of transfer learning for knowledge sharing over utilizing the information from source or target domain only. For each of the transfer learning algorithms we need to tune the hyper-parameters to achieve a reasonable tradeoff between the prior knowledge from the training dataset and the developing data samples (Fig. 2). Furthermore, the number of features selected for modeling also needs to be selected as a hyper-parameter for W-OMP (Fig. 2c). These hyper-parameters are selected using leave-one-out cross validation (LOOCV) on the developing data samples. As the base model is trained under ElasticNet regularization, the coefficients corresponding to the less-important features are shrunk to 0, which provide no prior knowledge to the transfer learning algorithms. In BMF, this issue can be tackled using two methods: 1) exclusively updating the non-zero model coefficients, and 2) learning the features without any prior knowledge and relying solely on data samples from the target domain. In this work, we train the BMF model using the second approach since it can help explore the impact of the factors with substantially higher importance in the target domain compared with the source domain, thereby recognizing the state transition. However, we also implement the first approach, which is referred to as BMF without the Missing Prior (BMF-W) for comparison, to demonstrate the efficacy to explore the features with zero coefficients from ElasticNet.

Figs. 3a and b show the hyper-parameter selection of BMF and W-OMP, respectively. The hyper-parameter of BMF, η, represents the importance of pre-trained base model. W-OMP requires two hyper-parameters (α and λ), which represent the tradeoff between two datasets and the number of selected features, respectively (Fig. 2). We generate five random splits of developing/testing parts on the secondary testing dataset and run the experiments in five trials accordingly. Taking the first trial as an example, the optimal parameters are selected as $\eta = e^{18.24}$ for BMF (Fig. 3a) and $\alpha =$ 6.28 billion, $\lambda = 3$ for W-OMP (Fig. 3b). As shown in the experimental results, the testing RMSE of the ElasticNet model is 295.22. We can also observe that the OMP algorithm can significantly improve the prediction performance and has an average test RMSE of 241.61 when the number of training samples increases from 6 to 10. Impressively, the lowest RMSE sharply declines to 179.93 when 10 data samples are used for training, which indicates OMP is a strong baseline model as one of the state-of-the-art algorithms for sparse data [59]. Compared with these baselines, the BMF method significantly outperforms both of them with an average

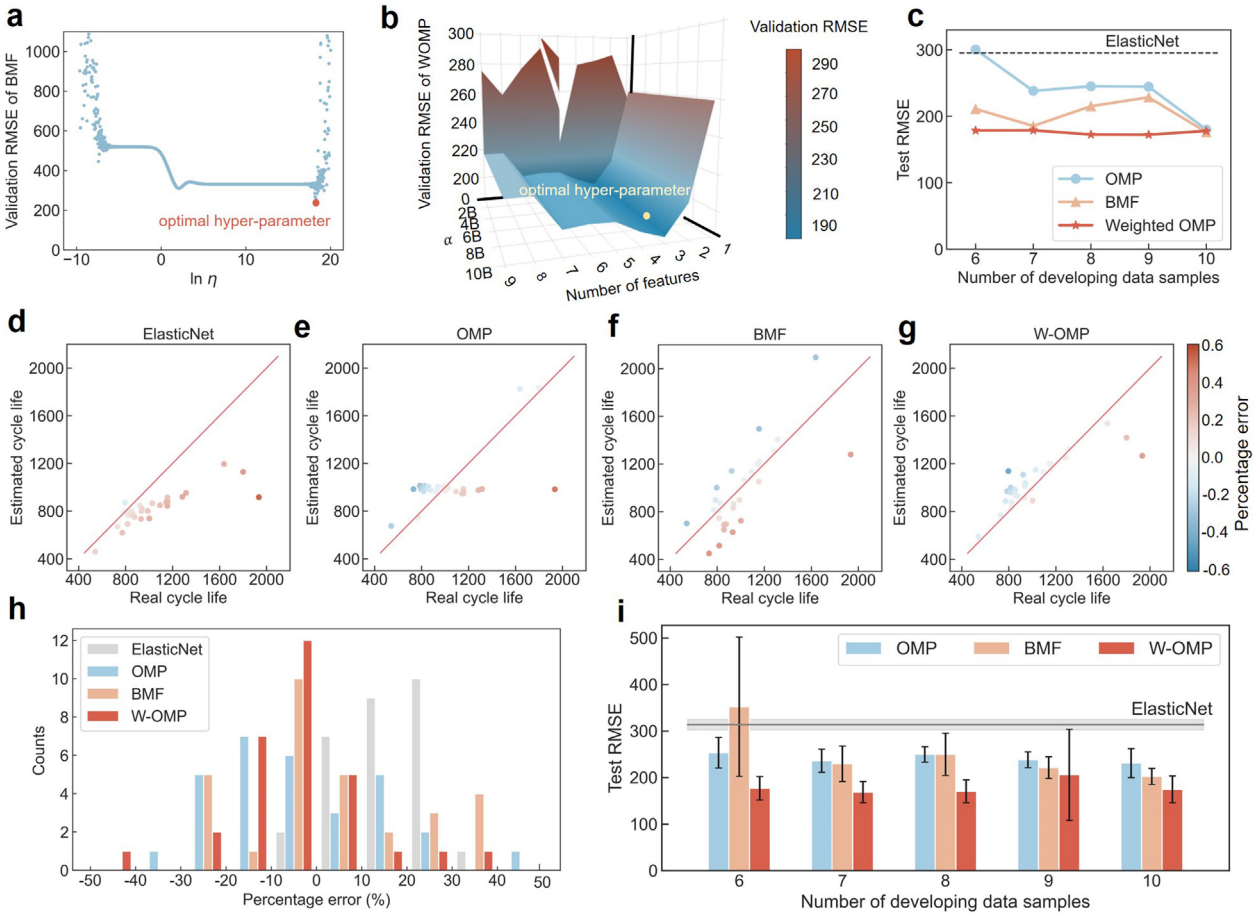

Fig. 3. Results. (a) The validation RMSE of BMF for cycle life prediction. The optimal ln η = 18.24 in the first trial of experiments. (b) The validation RMSE of W-OMP for cycle life prediction. On the axis corresponding to the value of α, the capital letter B stands for billion. The optimal hyper-parameters are $\alpha = 6.28 \times 10^9$ with 3 features in the first trial of experiments. (c) The testing RMSE of estimated cycle life versus real cycle life from ElasticNet, OMP, Bayesian model fusion and W-OMP in the first trial. Test results of estimated capacity versus real capacity by (d) ElasticNet, (e) OMP, (f) BMF, and (g) W-OMP. (h) The percentage error of algorithms when using eight developing data samples. (i) The average test RMSE with one standard deviation summarized from five trials.

RMSE of 203.16 and the lowest RMSE of 176.06. Furthermore, W-OMP performs the best with an average RMSE of 175.93 and the lowest RMSE of 172.14, and the prediction power remains stable across 6 to 10 developing data samples (Fig. 3c).

To better understand the predictions generated in the first trial, Figs. 3d–h visualize the predicted cycle life against the true values and the percentage errors for ElasticNet, OMP, BMF, and W-OMP when 8 data samples from developing part are utilized. ElasticNet tends to underestimate the cycle life and produce negative percentage errors, as many data points are located below the diagonal. On the contrary, overestimation occurs for OMP with more positive percentage errors. Our transfer learning algorithms (BMF and W-OMP) intelligently extract information from both resource and target domains to avoid estimation bias, and hence, their percentage errors are approximately normally distributed with a mean around zero (Fig. 3h). Furthermore, the percentage error of W-OMP is well controlled as the majority distributes within the range from −10% to 10%, which has smaller variability than BMF and therefore makes better predictions. We summarize the modeling accuracy of all trials in Fig. 3i to validate the robustness of proposed methods, and the error bars (one standard variation of the test RMSE) are shown to demonstrate the reliability of model predictions [60, 61]. Similar observations have been made as the first trial, such that W-OMP still performs the best, and BMF outperforms ElasticNet and OMP in those additional trials (Fig. 3i). A larger sample size is associated with a lower average testing RMSE and a better model robustness for BMF. For the scenarios with extremely few data samples, BMF cannot sufficiently catch the distribution of the target domain, thereby resulting in relatively large variations of test RMSE between trials. However, as the sample size increases, BMF could acquire more information from the target domain and quickly adapt to the new context, resulting in lower test RMSE compared to the baseline with stable performance across trials. If we use 10 data samples from the developing part, BMF-W has an average test RMSE of 228.52, which is 12.9% higher than BMF (average RMSE: 202.48, Supplementary Fig. 4). That is because BMF-W only re-assigns the weights of important features selected based on the training dataset. However, the importance of features may suffer from significant variations due to state transitions, which cannot be captured by BMF-W. In contrast, BMF can learn the weights of the features without prior knowledge using the information drawn from the developing part of secondary testing dataset, thereby leading to superior accuracy for prediction. Note that the improvement brought by transfer learning attributes to both incorporating extra knowledge and learning the appropriate approaches to utilize the incorporated knowledge. In order to demonstrate this, a new baseline is implemented, which trains a model based on all available source and target domain data without distinction using the OMP algorithm. In this comparison, the training dataset serves as the source domain data. We randomly shuffle the secondary testing dataset 100 times, and after each shuffle, we utilize the first 6 developing data samples as target domain data. In Supplementary Fig. 5, we present a visualization of the comparison between Unweighted OMP (U-OMP) and W-OMP, showcasing 20 cases where W-OMP outperforms U-OMP based on the corresponding test RMSE. With the same number of source

and target domain data across these 100 trials, W-OMP has a median test RMSE of 201.29, which outperforms the new baseline U-OMP (median RMSE: 212.24). This clearly demonstrates the advantage of the proposed transfer learning methods by optimizing the weighting between source and target domain information.

The explainability of the considered algorithms is investigated through analyzing the features selected for prediction and their importance in the corresponding models. The importance of each feature is measured using the average of absolute Shapley additive explanation (SHAP) values [62]. SHAP is an explanation machine learning technique that utilizes linear Local Interpretable Model-agnostic Explanations (LIME) [63] and game-theoretic approaches to identify the contribution of each attribute in the feature space to the final predictions. A feature may impact a prediction in either positive or negative way, and the mean absolute SHAP value shows us how much a single feature affects the predictions for a batch of data samples. For a linear model, the SHAP value of a specific feature is equal to the product of the feature's regression coefficient and the difference between the feature values and its own average [64]. Figs. 4a and d show the ranking of feature importance for ElasticNet, OMP, BMF, and W-OMP, respectively (F1–F9 are features extracted from the datasets, which their definition will be introduced in details in discussion section and can be found in Supplementary Table 1). ElasticNet and OMP select completely different sets of features since they are trained on datasets with different conditions. From these figures, we can observe that F2 is the most important feature of ElasticNet (mean absolute SHAP: 127.26, Fig. 4a), and F6, F8, and F4 are also included (mean absolute SHAP: 76.54, 26.84, and 14.94, respectively). OMP only selects F1 and F9 (mean absolute SHAP: 901.87 and 439.9, respectively, Fig. 4b). BMF outperforms the baseline models as it combines the top 2 features selected by ElasticNet (F2 and F6, mean absolute SHAP = 155.06 and 70.51) and the features selected by OMP (F1 and F9, mean absolute SHAP = 413.09 and 244.87; Fig. 4c), which reflect the important information in both source and target domains. Compared with OMP, the feature importance of F1 in BMF decreased due to its multi-collinearity with F2 (Pearson's correlation = 0.997) in the training dataset. W-OMP selected F3 and F5 (mean absolute SHAP: 74.59 and 49.95, respectively), which have not been selected as important features in aforementioned methods (Fig. 4d), besides F2. To disentangle the discrepancy between the feature extraction mechanisms of proposed algorithms, we visualize the Pearson's correlations between features and cycle life in the training dataset and secondary testing dataset in Figs. 4e and f, respectively, which can be viewed as the "ground truth". Under ideal situations, features with a high Pearson's correlation with the cycle life are regarded as key features and should be included in the models. For ElasticNet, the top chosen features (F2, F6, and F8) have very high Pearson's correlations with the cycle life in the training dataset (Fig. 4e). In contrast, F9, F3, and F5 are included in OMP or W-OMP, while none of them seems to have a strong correlation with cycle life in both training dataset and secondary testing dataset (Figs. 4e and f). Therefore, we would like to further explore the reason why these features are selected associated with both the scheme of OMP-based algorithms and the electrochemistry in lithium-ion batteries in the Discussion section.

3. Discussion

We now analyze and reveal the relationship between algorithms, datasets, and their choice of features. ElasticNet and OMP are the baseline models trained on training dataset and secondary testing dataset, respectively. ElasticNet selects F2, F6, F8 and F4 as the key features, while OMP chooses F1 and F9. Compared with these baselines, BMF obtains a more accurate prediction since it simultaneously considers the knowledge provided by two datasets to extract the key features with high importance in the OMP and ElasticNet models, respectively. As shown in Fig. 4c, this method selects the most important features (F9, F2, F1, F6) selected by ElasticNet (F2 and F6) and OMP (F1 and F9). However, instead of using data directly, the knowledge of training dataset is abstracted as a pre-trained model, so BMF may fail to capture key features that represent the essential differences between training dataset and secondary testing dataset, such as F5. On the other hand, W-OMP balances the importance of two data sources by directly utilizing the data and hence includes F2, F3, and F5 as the key features. F1 and F2 are extracted from the capacity–voltage curve and mainly concern about the voltage decay of batteries, so they have a strong correlation on both datasets (training dataset: 0.996; secondary testing dataset: 0.997, Fig. 5a, Supplementary Fig. 6). F3 refers to the capacity degradation rate in the early cycling, and F9 is the difference in internal resistance between cycle 100 and cycle 2 (Supplementary Table 1). Solid electrolyte interphase (SEI) growth usually occurs during the early cycling, which causes loss of lithium inventory and the internal resistance changes in battery. Thus, F3 and F9 have similar data distributions with a high

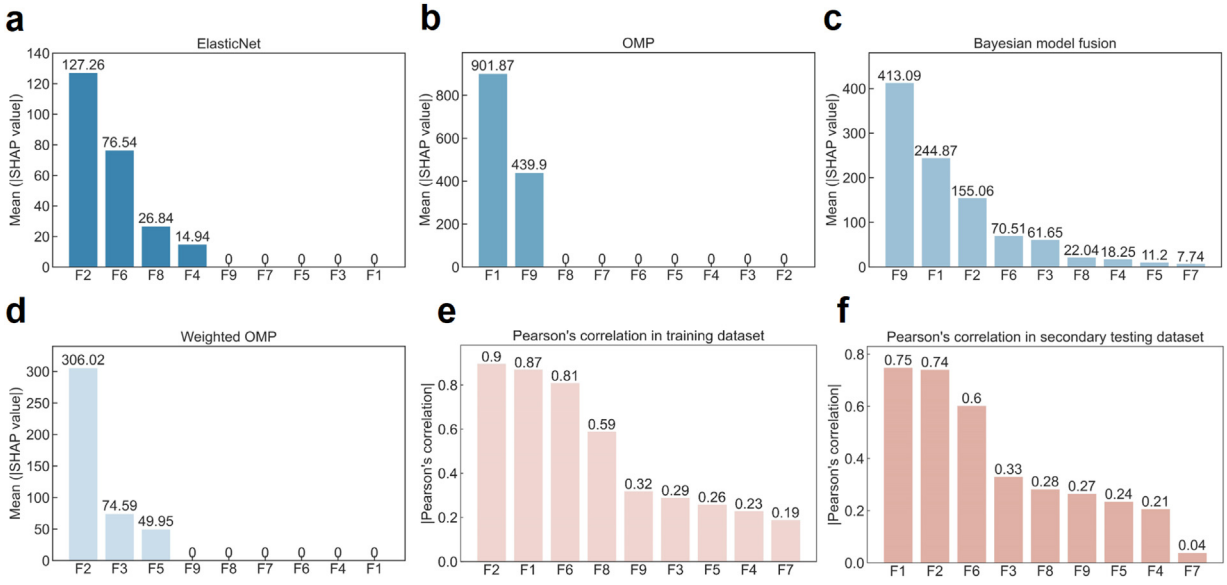

Fig. 4. Feature importance ranking in algorithms and datasets (a) The Shapley Additive explanation (SHAP) values of ElasticNet; (b) OMP; (c) Bayesian model fusion; (d) Weighted OMP; (e) The Pearson's correlation between each feature and cycle life in the training dataset; (f) The Pearson's correlation between each feature and cycle life in secondary testing dataset.

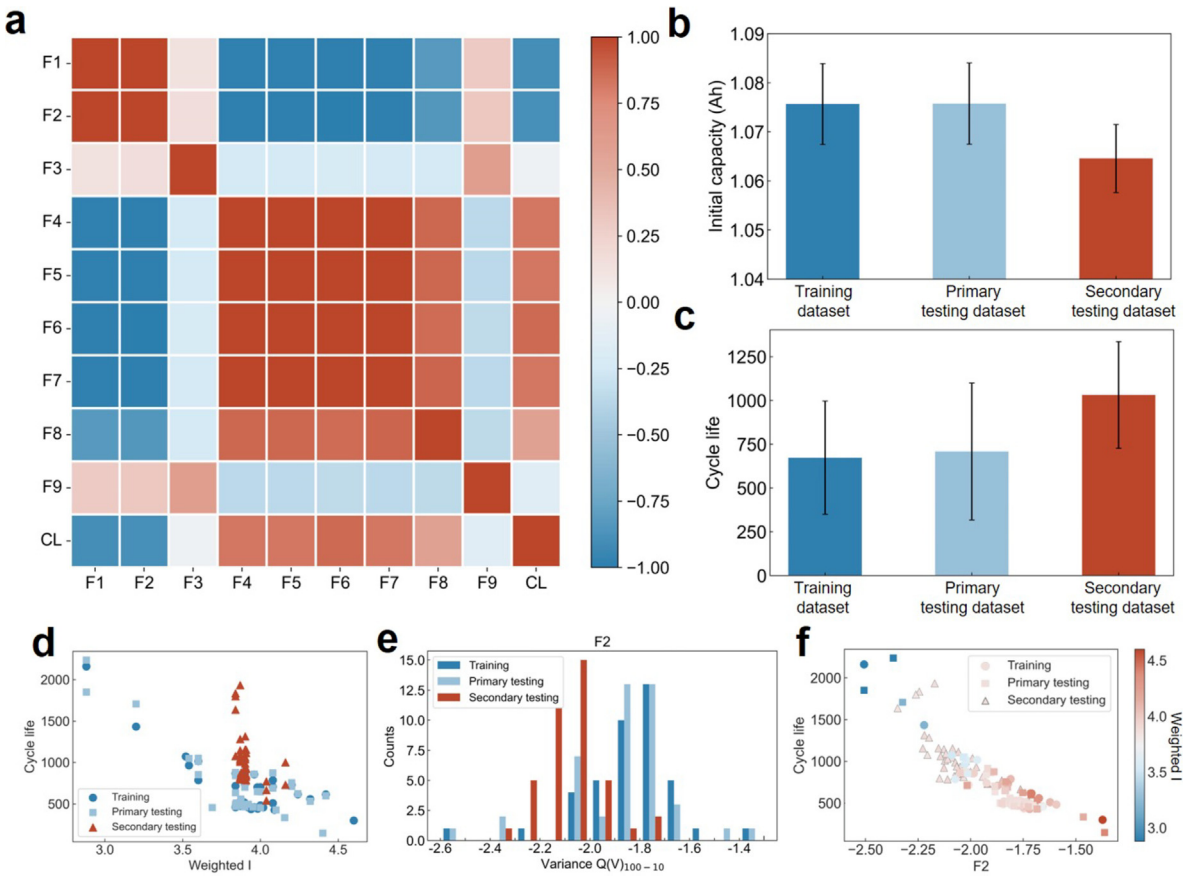

Fig. 5. Analysis and interpretation of key features selected by proposed algorithms (a) The Pearson's correlation between cycle life and each feature from the combination of training dataset and secondary testing dataset, in which the training dataset is scaled by the optimal weight from Weighted OMP. CL stands for "cycle life". (b) Discharge capacity at 2nd cycle (F5), and (c) cycle life of battery in different datasets. (d) Relationship between Weighted I and cycle life. (e) Distribution of F2 in different datasets. (f) Overview of F2, Weighted I and cycle life.

Pearson's correlation of 0.6 (Supplementary Figs. 7a and 7b, 8). In conclusion, BMF and W-OMP have successfully selected features that reflects the characteristics of the two algorithms and datasets, and demonstrated significantly improved prediction accuracy compared with ElasticNet. However, only W-OMP captures F5 since W-OMP could directly utilize the data from training dataset and the secondary testing dataset, and balance the weights between them.

F5 is defined as the discharge capacity (cycle 2) of batteries, which describes the battery aging state between datasets in a straightforward manner. Compared to training dataset and primary testing dataset, secondary testing dataset has significantly smaller F5 values (Fig. 5b, Supplementary Fig. 1) due to its approximately one-year extra storage time, inducing the calendar aging. Calendar aging experiences slow self-discharge aging of battery in open circuit state [54,65]. During this process, active lithium (lithiated graphite) slowly reacts with electrolyte and electrode materials under slow self-discharging condition, which continuously builds up SEI on electrode surface and causes battery aging [66–69]. Under ideal storage conditions, the battery capacity slowly decreases, and electrolyte solvent gradually forms passivation interphase in negative electrode [70]; as storage time increases, electrolyte can uniformly infiltrate on battery interfaces across multiple length scales, forming excellent SEI [71,72]. According to previous findings [55,73], long storage time or low current formation during early-stage charging significantly reduces SEI's charge transfer resistance, resulting in uniform and stable SEI and better cycling performance [73,74]. This agrees well with our observation among the three datasets, which the aged cells in the secondary dataset are with lower capacity increasement and prolonged cycle life (Supplementary Fig. 9, Fig. 5c). SEI growth is accompanied by the consumption of active lithium and thereby reduces the initial capacity, matching with the average lowest initial capacity in secondary testing dataset among three datasets (Fig. 5b). Furthermore, the capacity degradation rate (F3) in secondary testing dataset is lower than other two datasets (Supplementary Fig. 7a, Supplementary Table 1), which agrees with extremely small loss of active lithium and excellent SEI on negative electrode [72]. The high-quality SEI enhances the cycling performance and extends battery cycle life.

Apart from F5, we observed other phenomena that distinct batteries in secondary dataset from those in training and primary datasets. The three datasets have diverse calendar aging conditions and 72 different charging protocols. We develop a novel indicator, *Weighted I*, as weighted average charging rate to quantify the impacts of charging protocols on various features and datasets. The *Weighted I* is defined as the weighted average charging rate at 0–80% SOC, which is equal to $C_1 \times Q_1 + C_2 \times Q_2$. Fig. 5d shows that the *Weighted I* have profound effects on cycle life for inadequate aging batteries (training and primary datasets), but sufficient aging (secondary datasets) would mitigate such effects. Those findings show the distinct difference between the three datasets, and further validate the benefits of appropriate aging on prolonging cycle life. F2 depicts the electrochemical side reactions inside battery [75] and clearly shows the degradation state of lithium iron phosphate battery during early cycling [26]. Secondary testing dataset has smaller F2 values than other datasets and reveals less battery degradation and longer cycle life (Fig. 5e, Supplementary Fig. 8). However, in contrast to *Weighted I*, the linear association between F2 and cycle life persists across all the datasets (Fig. 5f), indicating F2 as a key feature for battery lifetime prediction. This is also why F2 and F1 are always chosen as key features in all algorithms applied in this research. The detailed analysis of other features indicating the different between secondary dataset and the other datasets is listed in the Supplementary Fig. 8.

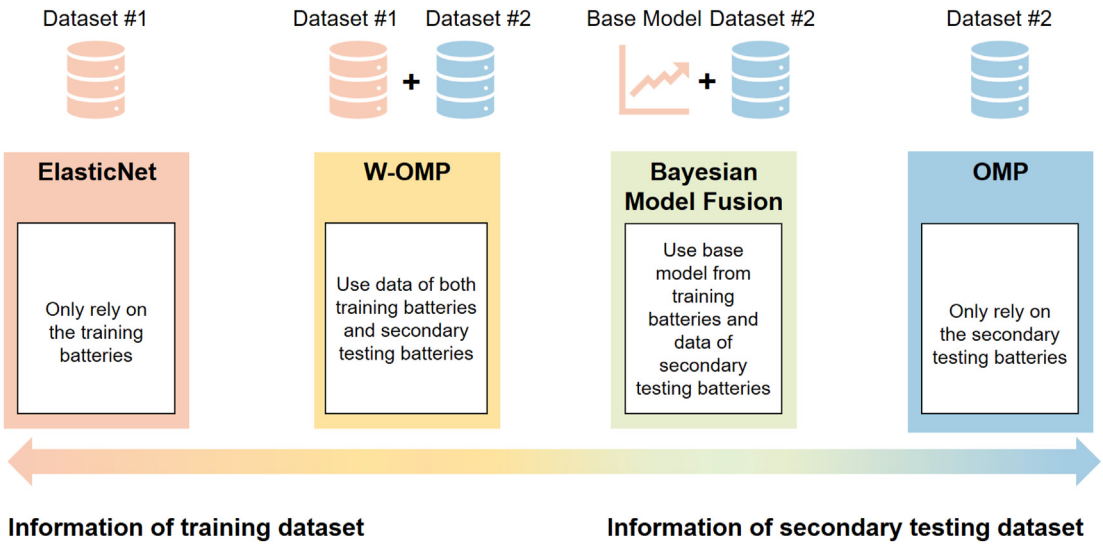

Fig. 6. The importance of information from training batteries and secondary test batteries for each algorithm.

In our work, we apply four algorithms to tackle different levels of data accessibility (Fig. 6). The test time of the secondary testing dataset was approximately 10–11 months later than the training dataset and primary testing dataset (Supplementary Fig. 2). ElasticNet or OMP are used if we have poor access to the data and only one battery dataset is available. Under the best scenario in which we have data from both batches, W-OMP is an ideal choice to balance the weights between two data sources. If we have the base model from the training dataset and data from the secondary testing dataset, we should apply BMF. We have also run BMF-W [53], which is a basic version of BMF algorithm mentioned before. However, BMF-W produces a testing RMSE near 229 across five trials using ten developing sample sizes, and the improvement on prediction accuracy is inferior to that of BMF (Supplementary Fig. 5). That is because BMF-W only re-assigns the weights of important features from the source domain, while BMF can incorporate extra dominating factors from the target domain to include more information. Hence, the BMF method should be preferred over BMF-W.

There are primarily two limitations in our proposed transfer learning methods. Firstly, our methods require obtaining external data from the target domain, which cannot be ensured in every scenario. Secondly, our algorithms initially incorporate all features from the external data and subsequently select the optimal ones; however, certain features from the external data might adversely affect predictions due to measurement errors or biases. For these features, we expect to learn their weights on target domain data only, which is not supported in the algorithms proposed in this work. In our future work, we would like to resolve those two limitations and enhance the robustness of our transfer learning framework. A major advantage of the proposed methods is the strong real-world applicability and high interpretability of linear models, which showcase satisfactory predictive performance when data samples are limited. To compare various methods on computational efficiency, scalability, and real-world applicability, we randomly shuffle the secondary testing data of MIT-Stanford datasets [26], while 10 and 30 data samples in the dataset are used for training and testing in each random trial. Under this setup, we validate the predictive performance of deep learning models, tree-based models, gaussian process regression, and linear models and summarize the characteristics of each method in Supplementary Table 2. Among these methods, linear models showcase computational advantages and the lowest peak memory usage (0.03 Mb for one trial). Due to the low computational cost and high real-world applicability, linear models are capable of being integrated into real-world Battery Management Systems for battery lifetime prediction [76]. Compared to some "black-box" deep learning-based methods that can usually achieve superior prediction accuracy, our proposed methods are directly established based on features with stronger interpretability, which can help us to disentangle the underlying physical mechanisms behind the state transitions [26,77]. With only ten training samples, the linear models outperform all other aforementioned methods, making them the ideal choice for battery lifetime prediction under limited data size (Supplementary Table 2). Another strength of these algorithms is their high adaptability to deep neural networks. Essentially, deep neural networks for predicting battery lifetime can be viewed as linear regression models, using the output from hidden layers as input features. While the proposed transfer learning algorithms can be applied to update the weights of hand-crafted features, they can also accommodate features automatically extracted using deep neural networks. In other words, the proposed transfer learning algorithms are not restricted to linear regression models; they offer a versatile framework that can accommodate various model architectures. Thirdly, the proposed methods are tailored to various levels of data accessibility, which not only satisfies the mathematical rigor but also provides enough flexibility for solving real-world applications.

4. Conclusions

In this work, transfer learning approaches are investigated for battery life prediction under state transitions to achieve superior prediction accuracy as well as excellent explainability. In specific, we developed two transfer learning methods, BMF and W-OMP, to strategically combine the prior knowledge provided by a related task with limited information extracted from the target dataset to achieve a superior prediction performance compared to using each dataset individually. Apart from improving the modeling accuracy, the explainability of these models is studied through analyzing the impactful features for battery lifetime prediction. Experiments are conducted on public datasets created using commercial lithium-ion batteries, where we found that the transfer learning methods can reduce the prediction RMSE by up to 41% through adapting to the target domain from either model or data perspective. Furthermore, it is also demonstrated that the transfer learning strategy can help identify the variations of impactful features across set of batteries, which provides novel insights for disentangling the battery degradation mechanisms and the root cause of state transitions from the perspective of data mining. Those findings suggest that transfer learning strategy used in our work has an outstanding capability to acquire knowledge across multiple data sources for solving specialized issues. In general, our transfer learning methods can complement or

integrate with electrochemical-based approaches to accurately predict the lifetime of lithium-ion batteries under state transitions.

5. Methods

The dataset used in this work is adopted from Severson et al. [26]. The dataset includes a total of 124 cylindrical LFP/graphite A123 APR18650M1A batteries with 72 fast charging protocols, which their discharging rate is 4C. The nominal capacity of these batteries is 1.1 Ah and the average lifetime is 806 cycles (ranging from 150 to 2300). It consists of three sub-datasets, including training dataset, primary testing dataset, and secondary testing dataset with 41, 43, and 40 batteries, respectively. The primary testing and training datasets consist of a fusion of data from Batch1 (batteries tested by 05/12/2017) and Batch2 (batteries tested by 06/30/2017). The disparity in calendar aging between these datasets is negligible. Furthermore, the charging protocols employed in both the primary testing and training datasets exhibit substantial similarities. In contrast, the secondary dataset was gathered at a significantly later date (04/12/2018), and the charging protocols employed demonstrate a narrower range of charging rates. Consequently, the inclusion of the primary testing dataset in our study is unnecessary since the training and secondary datasets adequately address the objectives of our research. The features for lifetime prediction are computed using the measurements obtained from the first 100 charge–discharge cycles. In this work, we consider 9 features denoted by F1 to F9 (details listed in Supplementary Table 1), which are extracted from capacity–voltage curve (Supplementary Fig. 10), discharge capacity fade curve (Supplementary Fig. 11), and other measurements (e.g. temperature and internal resistance, Supplementary Fig. 12).

The charging protocols are shown in Fig. 1d via three steps. The initial charging rate (C1) would change into C2 if the state of charge (SOC) reaches a designated level (Q1); after the SOC reaches 80%, it would start galvanostatic charging at 1C to 3.6 V and then changes to potentiostatic charging until fully charged, where a 1C charge rate represents the battery is fully charged in one hour, corresponding to a charging current of 1.1 A. The data distribution of C1 and Q1 are presented in Figs. 1e and f, respectively. The training dataset and primary testing dataset have similar charging protocols, while charging protocols in the secondary testing dataset have significant differences. As these three batches of batteries are maintained and measured under different conditions, the prediction model trained using one dataset cannot guarantee to have an equally high accuracy on another one, which can be observed from the experimental results in previous work [26]. Therefore, two individual transfer learning algorithms, i.e., BMF and W-OMP, are developed to efficiently utilize the knowledge provided by the training dataset (prior knowledge) and strategically combine it with the limited information extracted from the target testing dataset (observations) to achieve a superior performance. In this work, the prior knowledge is provided by the training dataset and the observations are drawn from the developing part of the secondary testing dataset. Furthermore, our proposed linear-based transfer learning algorithms have excellent performance across multiple criterions including accuracy, computation time, scalability, explainability, and real-world applicability when compared to conventional methods, such as electrochemical models, deep learning models (i.e., Neural Network), tree-based models (i.e., lightGBM), and Gaussian process regression (Supplementary Table 2).

BMF is developed for the scenario where only the base model trained on a related dataset is accessible. In this work, the base model is a linear regression model represented by the coefficient vector W_E such that the lifetime for a batch of batteries can be computed by $\widehat{Y} = XW_E$, where $\widehat{Y}$ is a column vector and each row of the matrix X represent the feature vector of the corresponding battery. As a common practice, we normalize each input feature and the label, such that their mean and variance on the training data are 0 and 1, before fitting the linear regression model. Hence, the intercept of the model is 0, and we only consider the coefficients corresponding to input features. The BMF algorithm intends to fine-tune the base model and achieve a late-stage linear regression model W_L using a set of data samples in the developing part of the secondary testing dataset, whose feature matrix and label vector are denoted by X_L and Y_L, respectively. The philosophy of BMF is to pose a prior distribution constraint on the late-stage model such that $W_L \sim N(W_E, I\lambda^2 W_E^2)$. Subsequently, a posterior distribution is formulated as

$$pdf(W_L|Y_L, X_L) \propto pdf(W_L) \times pdf(Y_L|W_L, X_L),$$

where $pdf(W_L)$ and $pdf(Y_L|W_L, X_L)$ are the probability density function (pdf)s of the prior distribution and likelihood, respectively. As a common routine for fitting a linear regression model, the likelihood for observing a dataset is assumed to follow Gaussian distribution, such that $Y_L|W_L$, $X_L \sim N(X_L W_L, I\sigma^2)$. Thus, the posterior distribution $pdf(W_L|Y_L, X_l)$ is also Gaussian, and hence, the maximum-a-posterior (MAP) estimation of W_L is equal to the mean of the posterior distribution as

$$W_L = \Sigma_L \left[\eta \cdot \left[W_{E,1}^{-1}, \ldots, W_{E,M}^{-1}\right]^T + X_L^T Y_L\right],$$

where $\Sigma_L = [\eta \cdot diag(W_{E,1}^{-2}, \ldots, W_{E,M}^{-2}) + X_L^T X_L]^{-1}$ is the covariance matrix. The hyper-parameter η represents the importance of early-stage weights and can be selected using LOOCV.

In contrast to utilizing only the base model, the W-OMP algorithm is proposed to directly learn from the raw data in both the source and target domain, to fit a linear regression model that strategically combines the knowledge from these datasets. Let the dataset used to train the base model be denoted by $\{X_E, Y_E\}$, where X_E and Y_E are the feature matrix and label vector, respectively. Given the set of data $\{X_L, Y_L\}$ sampled from the developing part of the secondary testing dataset, it aims to learn the model W_L that satisfies

$$\min \alpha \cdot \|X_E W_L - Y_E\|_2^2 + \|X_L W_L - Y_L\|_2^2 \; s.t. \; \|W_L\|_0 \leq \lambda,$$

where α controls the tradeoff of importance between the data from the source and target domains. While the optimization of model parameters can be formulated using MAP for BMF, the formulation of W-OMP can be derived using maximum likelihood estimation (MLE). The statistical foundation of W-OMP is presented in the Supplementary information. The L0-norm constraint $\|W_L\|_0 \leq \lambda$ indicates that the number of non-zero elements in W_L is at most λ, which encourages the algorithm to select a subset of important features for modeling, thereby avoiding overfitting. As both α and λ are hyper-parameters, we select them using the LOOCV method. Given a fixed value α and a subset of selected features Ω, W_L can be analytically computed as

$$W_L = \left[\alpha \cdot X_{E,\Omega}^T X_{E,\Omega} + X_{L,\Omega}^T X_{L,\Omega}\right]^{-1} \left[\alpha \cdot X_{E,\Omega}^T Y_E + X_{L,\Omega}^T Y_L\right],$$

where $X_{E,\Omega}$ and $X_{L,\Omega}$ are the feature matrices consisting of the columns corresponding to Ω in X_E and X_L. Similar to the standard OMP algorithm, the feature selection of W-OMP is conducted iteratively. It initializes Ω as an empty set and include the feature maximally correlated with the label in each iteration. After a new feature is selected, the labels are updated by subtracting the contribution of the selected feature before next iteration. Considering the tradeoff between the source and target domains, the importance of a feature j is measured by

$$\left|\alpha \cdot X_{E,j}^T Y_E + X_{L,j}^T Y_L\right|,$$

which represents their linear correlation considering the weighting of data samples from the source and target domains, and the W-OMP algorithm terminates after $|\Omega| = \lambda$, which means that the required number of features have been selected.

Author contributions

Tianze Lin: Writing – review & editing, Writing – original draft, Visualization, Project administration. **Sihui Chen:** Writing – review & editing, Writing – original draft, Visualization, Project administration. **Stephen J. Harris:** Writing – review & editing. **Tianshou Zhao:** Writing – review & editing. **Yang Liu:** Writing – review & editing, Supervision, Methodology, Conceptualization. **Jiayu Wan:** Writing – review & editing, Supervision, Methodology, Conceptualization.

Declaration of competing interest

The authors declare no competing interests.

Acknowledgments

This work is supported by the startup fund of Shanghai Jiao Tong University and Southern University of Science and Technology. S.J.H is supported by the Laboratory Directed Research and Development Program of Lawrence Berkeley National Laboratory under U.S. Department of Energy contract no. DE-AC02-05CH11231.

Appendix A. Supplementary data

Supplementary data to this article can be found online at https://doi.org/10.1016/j.esci.2024.100280.

References

[1] X.-B. Cheng, R. Zhang, C.-Z. Zhao, Q. Zhang, Toward safe lithium metal anode in rechargeable batteries: a review, Chem. Rev. 117 (2017) 10403–10473.
[2] B. Anasori, M.R. Lukatskaya, Y. Gogotsi, 2D metal carbides and nitrides (MXenes) for energy storage, Nat. Rev. Mater. 2 (2017) 1–17.
[3] K. Xu, Nonaqueous liquid electrolytes for lithium-based rechargeable batteries, Chem. Rev. 104 (2004) 4303–4418.
[4] Y. Zhang, Y. Li, Z. Guo, J. Li, X. Ge, Q. Sun, Z. Yan, Z. Li, Y. Huang, Health monitoring by optical fiber sensing technology for rechargeable batteries, eScience 4 (2023) 100174.
[5] G. Harper, R. Sommerville, E. Kendrick, L.O. Driscoll, P.R. Slater, R. Stolkin, A. Walton, P.T. Christensen, O. Heidrich, S. Lambert, A. Abbott, K.S. Ryder, L. Gaines, P. Anderson, Recycling lithium-ion batteries from electric vehicles, Nature 575 (2019) 75–86.
[6] Z. Chen, D. Banham, S. Ye, A. Hintennach, J. Lu, M.C. Fowler, Z.P. Cano, Batteries and fuel cells for emerging electric vehicle markets, Nat. Energy 3 (2018) 279–289.
[7] C. Liu, Y. Li, D. Lin, P.-C. Hsu, B. Liu, G. Yan, T. Wu, Y. Cui, S. Chu, Lithium extraction from seawater through pulsed electrochemical intercalation, Joule 4 (2020) 1459–1469.
[8] T.M. Gür, Review of electrical energy storage technologies, materials and systems: challenges and prospects for large-scale grid storage, Energy Environ. Sci. 11 (2018) 2696–2767.
[9] P. Barpanda, G. Oyama, S. Nishimura, S.-C. Chung, A. Yamada, A 3.8-V earth-abundant sodium battery electrode, Nat. Commun. 5 (2014) 4358.
[10] Z. Yang, J. Zhang, M.C.W. Kintner-Meyer, X. Lu, D. Choi, J.P. Lemmon, J. Liu, Electrochemical energy storage for green grid, Chem. Rev. 111 (2011) 3577–3613.
[11] H. Wang, Z. Yu, X. Kong, W. Huang, Z. Zhang, D.G. Mackanic, X. Huang, J. Qin, Z. Bao, Y. Cui, Dual-solvent Li-ion solvation enables high-performance Li-metal batteries, Adv. Mater. 33 (2021) 2008619.
[12] Y. Wang, C. Chen, H. Xie, T. Gao, Y. Yao, G. Pastel, X. Han, Y. Li, J. Zhao, K. (Kelvin) Fu, L. Hu, 3D-printed all-fiber Li-ion battery toward wearable energy storage, Adv. Funct. Mater. 27 (2017) 1703140.
[13] S. Sharifi-Asl, J. Lu, K. Amine, R. Shahbazian-Yassar, Oxygen release degradation in Li-ion battery cathode materials: mechanisms and mitigating approaches, Adv. Energy Mater. 9 (2019) 1900551.
[14] Y. Yang, W. Yang, H. Yang, H. Zhou, Electrolyte design principles for low-temperature lithium-ion batteries, eScience 3 (2023) 100170.
[15] A. Masias, J. Marcicki, W.A. Paxton, Opportunities and challenges of lithium ion batteries in automotive applications, ACS Energy Lett. 6 (2021) 621–630.
[16] X. Hu, L. Xu, X. Lin, M. Pecht, Battery lifetime prognostics, Joule 4 (2020) 310–346.
[17] A.D. Sendek, Q. Yang, E.D. Cubuk, K.-A.N. Duerloo, Y. Cui, E.J. Reed, Holistic computational structure screening of more than 12000 candidates for solid lithium-ion conductor materials, Energy Environ. Sci. 10 (2017) 306–320.
[18] M. Kim, I. Kim, J. Kim, J.W. Choi, Lifetime prediction of lithium ion batteries by using the heterogeneity of graphite anodes, ACS Energy Lett. 8 (2023) 2946–2953.
[19] Z.M. Konz, E.J. McShane, B.D. McCloskey, Detecting the onset of lithium plating and monitoring fast charging performance with voltage relaxation, ACS Energy Lett. 5 (2020) 1750–1757.
[20] A. Kwade, W. Haselrieder, R. Leithoff, A. Modlinger, F. Dietrich, K. Droeder, Current status and challenges for automotive battery production technologies, Nat. Energy 3 (2018) 290–300.
[21] A.A. Franco, A. Rucci, D. Brandell, C. Frayret, M. Gaberscek, P. Jankowski, P. Johansson, Boosting rechargeable batteries R&D by multiscale modeling: myth or reality? Chem. Rev. 119 (2019) 4569–4627.
[22] P.M. Attia, A. Grover, N. Jin, K.A. Severson, T.M. Markov, Y.H. Liao, M.H. Chen, B. Cheong, N. Perkins, Z. Yang, P.K. Herring, M. Aykol, S.J. Harris, R.D. Braatz, S. Ermon, W.C. Chueh, Closed-loop optimization of fast-charging protocols for batteries with machine learning, Nature 578 (2020) 397–402.
[23] Z. Wang, Z. Sun, H. Yin, H. Wei, Z. Peng, Y.X. Pang, G. Jia, H. Zhao, C.H. Pang, Z. Yin, The role of machine learning in carbon neutrality: catalyst property prediction, design, and synthesis for carbon dioxide reduction, eScience 3 (2023) 100136.
[24] Y. Zhang, Q. Tang, Y. Zhang, J. Wang, U. Stimming, A.A. Lee, Identifying degradation patterns of lithium ion batteries from impedance spectroscopy using machine learning, Nat. Commun. 11 (2020) 1706.
[25] M.-F. Ng, J. Zhao, Q. Yan, G.J. Conduit, Z.W. Seh, Predicting the state of charge and health of batteries using data-driven machine learning, Nat. Mach. Intell. 2 (2020) 161–170.
[26] K.A. Severson, P.M. Attia, N. Jin, N. Perkins, B. Jiang, Z. Yang, M.H. Chen, M. Aykol, P.K. Herring, D. Fraggedakis, M.Z. Bazant, S.J. Harris, W.C. Chueh, R.D. Braatz, Data-driven prediction of battery cycle life before capacity degradation, Nat. Energy 4 (2019) 383–391.
[27] P.K. Jones, U. Stimming, A.A. Lee, Impedance-based forecasting of lithium-ion battery performance amid uneven usage, Nat. Commun. 13 (2022) 4806.
[28] Y. Li, K. Liu, A.M. Foley, A. Zülke, M. Berecibar, E. Nanini-Maury, J. Van Mierlo, H.E. Hoster, Data-driven health estimation and lifetime prediction of lithium-ion batteries: a review, Renew. Sustain. Energy Rev. 113 (2019) 109254–109254.
[29] Y. Wang, J. Tian, Z. Sun, L. Wang, R. Xu, M. Li, Z. Chen, A comprehensive review of battery modeling and state estimation approaches for advanced battery management systems, Renew. Sustain. Energy Rev. 131 (2020) 110015.
[30] C. Han, Y.-C. Gao, X. Chen, X. Liu, N. Yao, L. Yu, L. Kong, Q. Zhang, A self-adaptive, data-driven method to predict the cycling life of lithium-ion batteries, InfoMat 6 (2024) e12521.
[31] Z. Fei, F. Yang, K.L. Tsui, L. Li, Z. Zhang, Early prediction of battery lifetime via a machine learning based framework, Energy 225 (2021) 120205–120205.
[32] N. He, Q. Wang, Z. Lu, Y. Chai, F. Yang, Early prediction of battery lifetime based on graphical features and convolutional neural networks, Appl. Energy 353 (2024) 122048.
[33] N.H. Paulson, J. Kubal, L. Ward, S. Saxena, W. Lu, S.J. Babinec, Feature engineering for machine learning enabled early prediction of battery lifetime, J. Power Sources 527 (2022) 231127–231127.
[34] J. Tian, R. Xiong, W. Shen, J. Lu, X.G. Yang, Deep neural network battery charging curve prediction using 30 points collected in 10 min, Joule 5 (2021) 1521–1534.
[35] C.W. Hsu, R. Xiong, N.Y. Chen, J. Li, N.T. Tsou, Deep neural network battery life and voltage prediction by using data of one cycle only, Appl. Energy 306 (2022) 118134.
[36] C. Lea, M.D. Flynn, R. Vidal, A. Reiter, G.D. Hager, Temporal convolutional networks for action segmentation and detection, in: Proceedings of the IEEE Conference on Computer Vision and Pattern Recognition, 2017, pp. 1003–1012.
[37] B. Jiang, W.E. Gent, F. Mohr, S. Das, M.D. Berliner, M. Forsuelo, H. Zhao, P.M. Attia, A. Grover, P.K. Herring, M.Z. Bazant, S.J. Harris, S. Ermon, W.C. Chueh, R.D. Braatz, Bayesian learning for rapid prediction of lithium-ion battery-cycling protocols, Joule 5 (2021) 3187–3203.
[38] J. Zhu, Y. Wang, Y. Huang, R. Bhushan Gopaluni, Y. Cao, M. Heere, M.J. Mühlbauer, L. Mereacre, H. Dai, X. Liu, A. Senyshyn, X. Wei, M. Knapp, H. Ehrenberg, Data-driven capacity estimation of commercial lithium-ion batteries from voltage relaxation, Nat. Commun. 13 (2022) 2261.
[39] G. Ma, S. Xu, T. Yang, Z. Du, L. Zhu, H. Ding, Y. Yuan, A transfer learning-based method for personalized state of health estimation of lithium-ion batteries, IEEE Trans. Neural Netw. Learn. Syst. 35 (2022) 759–769.
[40] X. Shu, J. Shen, G. Li, Y. Zhang, Z. Chen, Y. Liu, A flexible state-of-health prediction scheme for lithium-ion battery packs with long short-term memory network and transfer learning, IEEE Trans. Transp. Electrif. 7 (2021) 2238–2248.
[41] Z. Deng, X. Lin, J. Cai, X. Hu, Battery health estimation with degradation pattern recognition and transfer learning, J. Power Sources 525 (2022) 231027.
[42] F. Feng, S. Teng, K. Liu, J. Xie, Y. Xie, B. Liu, K. Li, Co-estimation of lithium-ion battery state of charge and state of temperature based on a hybrid electrochemical-thermal-neural-network model, J. Power Sources 455 (2020) 227935–227935.
[43] K. Weiss, T.M. Khoshgoftaar, D. Wang, A survey of transfer learning, J. Big Data 3 (2016) 9.
[44] F. Zhuang, Z. Qi, K. Duan, D. Xi, Y. Zhu, H. Zhu, H. Xiong, Q. He, A comprehensive survey on transfer learning, Proc. IEEE 109 (2021) 43–76.
[45] Y. Che, Z. Deng, X. Lin, L. Hu, X. Hu, Predictive battery health management with transfer learning and online model correction, IEEE Trans. Veh. Technol. 70 (2021) 1269–1277.
[46] Y. Tan, G. Zhao, Transfer learning with long short-term memory network for state-of-health prediction of lithium-ion batteries, IEEE Trans. Ind. Electron. 67 (2020) 8723–8731.
[47] Z. Ye, J. Yu, State-of-health estimation for lithium-ion batteries using domain adversarial transfer learning, IEEE Trans. Power Electron. 37 (2022) 3528–3543.
[48] S.N. Lauro, J.N. Burrow, C.B. Mullins, Restructuring the lithium-ion battery: a perspective on electrode architectures, eScience 3 (2023) 100152.
[49] S. Pan, Q. Yang, A survey on transfer learning, Knowl. Data Eng. IEEE Trans. 22 (2010) 1345–1359.

[50] M. Alam, D. Buscaldi, M. Cochez, F. Osborne, D. Reforgiato Recupero, H. Sack, S. Monka, L. Halilaj, A. Rettinger, M. Alam, D. Buscaldi, M. Cochez, F. Osborne, D. Refogiato Recupero, H. Sack, A survey on visual transfer learning using knowledge graphs, Semant. Web 13 (2022) 477–510.
[51] L. Zhang, T. Xiang, S. Gong, Learning a deep embedding model for zero-shot learning, in: 2017 IEEE Conf. Comput. Vis. Pattern Recognit., CVPR, 2017, pp. 3010–3019.
[52] K. Liu, Q. Peng, Y. Che, Y. Zheng, K. Li, R. Teodorescu, D. Widanage, A. Barai, Transfer learning for battery smarter state estimation and ageing prognostics: recent progress, challenges, and prospects, Adv. Appl. Energy 9 (2023) 100117.
[53] F. Wang, P. Cachecho, W. Zhang, S. Sun, X. Li, R. Kanj, C. Gu, Bayesian model fusion: large-scale performance modeling of analog and mixed-signal circuits by reusing early-stage data, IEEE Trans. Comput. Aided Des. Integr. Circuits Syst. 35 (2016) 1255–1268.
[54] J. Schmitt, A. Maheshwari, M. Heck, S. Lux, M. Vetter, Impedance change and capacity fade of lithium nickel manganese cobalt oxide-based batteries during calendar aging, J. Power Sources 353 (2017) 183–194.
[55] A. Gismero, D.-I. Stroe, E. Schaltz, Calendar aging lifetime model for NMC-based lithium-ion batteries based on EIS measurements, in: 2019 Fourteenth International Conference on Ecological Vehicles and Renewable Energies, 2019, pp. 1–8.
[56] B.Q. Huynh, H. Li, M.L. Giger, Digital mammographic tumor classification using transfer learning from deep convolutional neural networks, J. Med. Imaging 3 (2016) 034501.
[57] L. Wang, B. Guo, Q. Yang, Smart city development with urban transfer learning, Computer 51 (2018) 32–41.
[58] X. Li, Finding deterministic solution from underdetermined equation: large-scale performance variability modeling of analog/RF circuits, IEEE Trans. Comput. Aided Des. Integr. Circuits Syst. 29 (2010) 1661–1668.
[59] Z. Gao, L. Dai, C. Hu, X. Gao, Z. Wang, Chapter 6 – Channel Estimation for mmWave Massive MIMO Systems, MmWave Massive MIMO, Academic Press, 2017, pp. 113–139.
[60] D. Morgan, R. Jacobs, Opportunities and challenges for machine learning in materials science, Annu. Rev. Mater. Res. 50 (2020) 71–103.
[61] Z. Wang, Z. Sun, H. Yin, X. Liu, J. Wang, H. Zhao, C.H. Pang, T. Wu, S. Li, Z. Yin, X.-F. Yu, Data-driven materials innovation and applications, Adv. Mater. 34 (2022) 2104113.
[62] S.M. Lundberg, S.-I. Lee, A Unified approach to interpreting model predictions, in: Proceedings of the 31st International Conference on Neural Information Processing Systems, 2017, pp. 4768–4777.
[63] M.T. Ribeiro, S. Singh, C. Guestrin, "Why should i trust you?" Explaining the predictions of any classifier, in: Proc. ACM SIGKDD Int. Conf. Knowl. Discov. Data Min, 2016, pp. 1135–1144.
[64] J. Park, H. Zhao, S.D. Kang, K. Lim, C.C. Chen, Y.S. Yu, R.D. Braatz, D.A. Shapiro, J. Hong, M.F. Toney, M.Z. Bazant, W.C. Chueh, Fictitious phase separation in Li layered oxides driven by electro-autocatalysis, Nat. Mater. 20 (2021) 991–999.
[65] I. Zilberman, S. Ludwig, A. Jossen, Cell-to-cell variation of calendar aging and reversible self-discharge in 18650 nickel-rich, silicon–graphite lithium-ion cells, J. Energy Storage 26 (2019) 100900.
[66] E. Peled, D. Golodnitsky, Chapter 1–SEI on lithium, graphite, disordered carbons and tin-based alloys. Lithium-ion batteries: solid-electrolyte interphase, World Scientific, 2004, pp. 1–69.
[67] N. Dupré, J.-F. Martin, J. Oliveri, P. Soudan, A. Yamada, R. Kanno, D. Guyomard, Relationship between surface chemistry and electrochemical behavior of $LiNi_{1/2}Mn_{1/2}O_2$ positive electrode in a lithium-ion battery, J. Power Sources 196 (2011) 4791–4800.
[68] S.-P. Kim, A.C.T. van Duin, V.B. Shenoy, Effect of electrolytes on the structure and evolution of the solid electrolyte interphase (SEI) in Li-ion batteries: a molecular dynamics study, J. Power Sources 196 (2011) 8590–8597.
[69] L. Wang, J. Qiu, X. Wang, L. Chen, G. Cao, J. Wang, H. Zhang, X. He, Insights for understanding multiscale degradation of $LiFePO_4$ cathodes, eScience 2 (2022) 125–137.
[70] E. Sarasketa-Zabala, I. Gandiaga, L. Rodríguez-Martínez, I. Villarreal, Calendar ageing analysis of a $LiFePO_4$/graphite cell with dynamic model validations: towards realistic lifetime predictions, J. Power Sources 272 (2014) 45–57.
[71] W. Bao, J. Wan, X. Han, X. Cai, H. Zhu, D. Kim, D. Ma, Y. Xu, J.N. Munday, H.D. Drew, M.S. Fuhrer, L. Hu, "Approaching the limits" of transparency and conductivity in graphitic materials through lithium intercalation, Nat. Commun. 5 (2014) 4224.
[72] J. Harlow, D. Stevens, J. Burns, J. Reimers, J. Dahn, Ultra high precision study on high capacity cells for large scale automotive application, J. Electrochem. Soc. 160 (2013) A2306–A2310.
[73] T. Zhu, Q. Hu, G. Yan, J. Wang, Z. Wang, H. Guo, X. Li, W. Peng, Manipulating the composition and structure of solid electrolyte interphase at graphite anode by adjusting the formation condition, Energy Technol. 7 (2019) 1900273.
[74] L. von Kolzenberg, M. Werres, J. Tetzloff, B. Horstmann, Transition between growth of dense and porous films: theory of dual-layer SEI, Phys. Chem. Chem. Phys. 24 (2022) 18469–18476.
[75] Z. Chen, D.L. Danilov, L.H.J. Raijmakers, K. Chayambuka, M. Jiang, L. Zhou, J. Zhou, R.-A. Eichel, P.H.L. Notten, Overpotential analysis of graphite-based Li-ion batteries seen from a porous electrode modeling perspective, J. Power Sources 509 (2021) 230345.
[76] M. Lelie, T. Braun, M. Knips, H. Nordmann, F. Ringbeck, H. Zappen, D.U. Sauer, Battery management system hardware concepts: an overview, Appl. Sci. 8 (2018) 534.
[77] F. Poursabzi-Sangdeh, D.G. Goldstein, J.M. Hofman, J.W. Wortman Vaughan, H. Wallach, Manipulating and measuring model interpretability, in: Proc. 2021 CHI Conf. Hum. Factors Comput. Syst., Association for Computing Machinery, 2021, pp. 1–52.